Chapter 5

Influence of flexoelectricity on the EHD instabilities in nematics : a one-dimensional linear analysis for AC excitation

CHAPTER 5

INFLUENCE OF FLEXOELECTRICITY ON THE EHD INSTABILITIES IN NEMATICS: A ONE-DIMENSIONAL LINEAR ANALYSIS FOR AC EXCITATION

5.1 INTRODUCTION

In this chapter we extend our calculations to the case of AC excitation. In order to simplify the analysis the boundary conditions are neglected. This model offers a satisfactory explanation of many experimental observations which cannot be accounted for by using the Helfrich [1] and Orsay models [2,3]. These include the oblique-roll instability observed at low frequencies in the conduction regime, the chevron pattern found in the dielectric regime and the low frequency EHD instability exhibited by nematics with a negative conductivity anisotropy [4,5,6] (see chapter 2, section 6).

5.2 THE ELECTROHYDRODYNAMIC EQUATIONS

We consider the same geometry as in the previous two chapters (Fig.1). Since the boundary conditions are neglected all the variables in the problem are functions of t and ξ only. The system is described by the following linearized equations.

1) The Poisson equation, $\text{div}\,\vec{D} = 4\pi Q$.

Substituting for $\vec{D}$ (see Eq.(6), chapter 1), we get

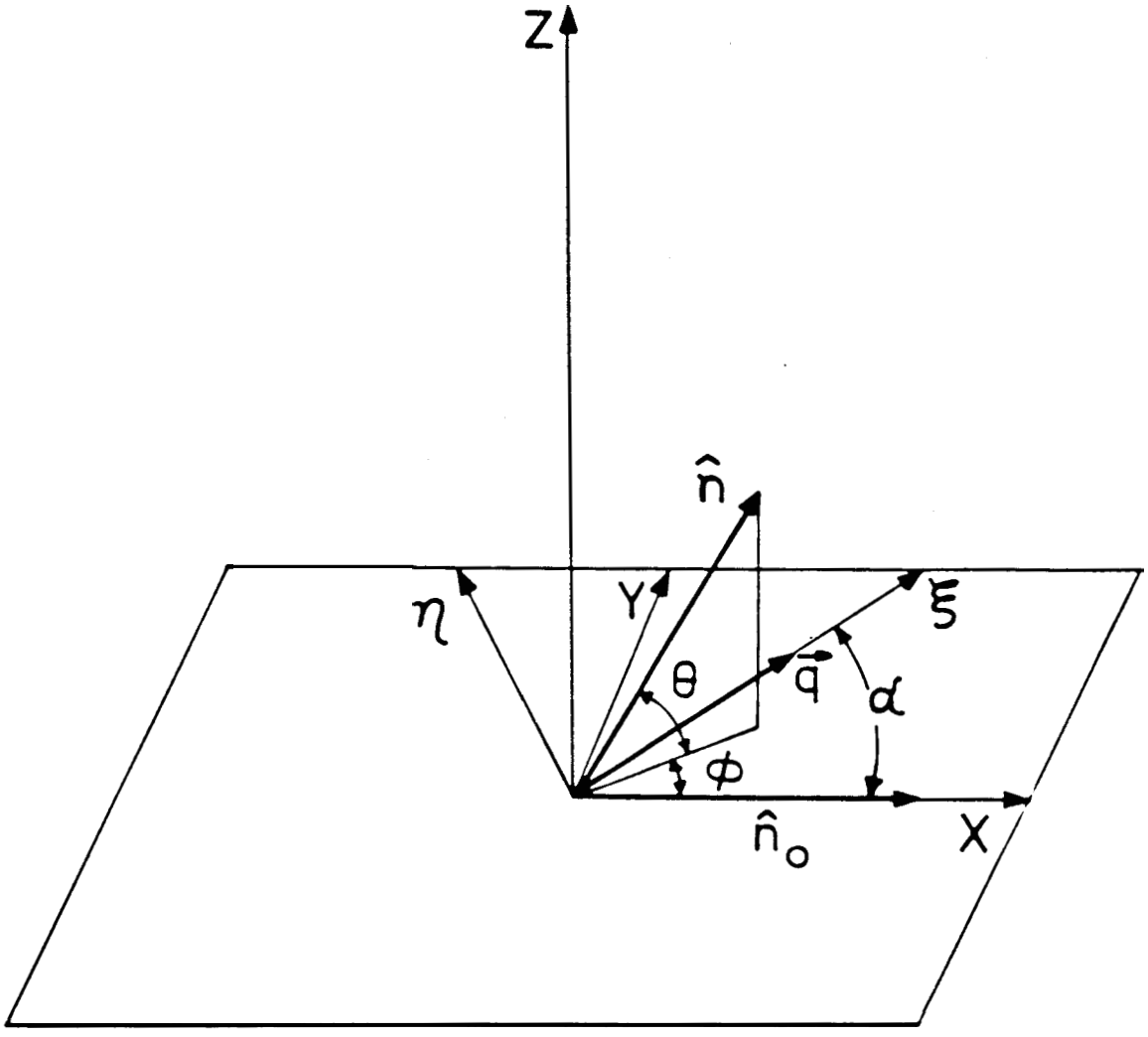

Fig.l. Illustration of the coordinate system and definitions of the angles used in the text.

$$4\pi Q = \epsilon_c \left(\partial E_\xi / \partial \xi\right) + \epsilon_a E_a c \left(\partial \theta / \partial \xi\right) + 4\pi (e_1 + e_3)\, s\, c \left(\partial^2 \Phi / \partial \xi^2\right) \qquad (1)$$

where, $\epsilon_c = \epsilon_\perp + \epsilon_a c$, $c = \cos a$, $s = \sin a$ and E_a is the applied field.

2) The charge continuity equation, $(\partial Q / \partial t) + \text{div}\ \vec{J} = 0$. Substituting for $\vec{J}$ (see Eq.(8), chapter 1), this equation leads to

$$(\partial Q / \partial t) + \sigma_c \left(\partial E_\xi / \partial \xi\right) + \sigma_a E_a c \left(\partial \theta / \partial \xi\right) = 0 \qquad (2)$$

where, $\sigma_c = a, + \sigma_a c$.

3) The equation of motion [2],

$$\rho \left(\partial \vec{v} / \partial t\right) + \text{div}\ (\rho \vec{v}\vec{v}) - \text{div}\ (\bar{\bar{\sigma}} + \bar{\bar{\sigma}}') = Q \vec{E}$$

Since we are considering a one-dimensional model only the Z-component of the velocity appears in the above equation. The inertial term in the above equation is negligible as long as the excitation frequency is not too large. Further, the elastic stress tensor $\bar{\bar{\sigma}}$ does not lead to any linear terms. Neglecting these two terms and substituting for the viscous stress tensor $\bar{\bar{\sigma}}'$, we get

$$a_2 c \left(\partial \dot{\theta} / \partial \xi\right) + \eta_1 \left(\partial^2 v_z / \partial \xi^2\right) + Q E_a = 0 \qquad (3)$$

where, $\dot{\theta} = \partial\theta/\partial t$ and $\eta_1 = \frac{1}{2}[\, a+ + (a_5 - a_2)\, c^2 \,]$.

4) The torque balance along Y yields

$$\gamma_1\dot{\theta} + a_2\, c\,(\partial v_z/\partial\xi) - M(\partial^2\theta/\partial\xi^2) - (\epsilon_a E_a^2/4\pi)\,\theta - (\epsilon_a c\, E_a/4\pi)E_\xi - (e_1 - e_3)E_a s\,(\partial\Phi/\partial\xi) = 0 \qquad (4)$$

where, $M = K_2 s^2 + K_3 c^2$.

5) The torque balance along Z gives

$$\gamma_1\dot{\Phi} + (e_1 - e_3)s\, E_a(\partial\theta/\partial\xi) - L(\partial^2\Phi/\partial\xi^2) + (e_1 + e_3)\, s\, c\,(\partial E_\xi/\partial\xi) = 0 \qquad (5)$$

where, $\dot{\Phi} = \partial\Phi/\partial t$ and $L = K_1 s^2 + K_3 c^2$.

Eliminating E_ξ and v_z from Eqs. (1-5), and assuming the solutions:

$\psi = \psi(t)\exp(iq\xi)$, $\Phi = \Phi(t)\exp(iq\xi)$ and $Q = Q(t)\exp(iq\xi)$,

where $\psi = (\partial\theta/\partial\xi)$, we get the following equations which describe the response of the system to the applied AC electric field.

$$\dot{\psi} + \psi/T_\psi + (\rho_1 E_a/\eta_2)\,\Phi + (A\, E_a/\eta_2)\, Q = 0 \qquad (6)$$

$$\dot{\Phi} + \Phi/T_\phi + (e_\psi E_a/\gamma_1)\,\psi + (e_\rho/\gamma_1)\, Q = 0 \qquad (7)$$

$$\dot{Q} + Q/\tau + \sigma_\psi E_a \psi + (\rho_2/\tau)\Phi = 0 \qquad (8)$$

where, $1/T_\psi = (M q^2 - \epsilon_\perp \epsilon_r E_a^2/4\pi)/\eta_2$, $A = -(\epsilon_r + a_2/\eta_1)c$, $\rho_1 = [(e_1 - e_3) - (e_1 + e_3)c^2\epsilon_r]s\, q^2$, $\eta_2 = (a_3 - a_2) - a_2^2 c^2/\eta_1$, $1/T_\phi = [L + 4\pi (e_1 + e_3)^2 s^2 c^2/\epsilon_c]\, q^2/(a_3 - a_2)$, $e_\rho = 4\pi (e_1 + e_3)\, s\, c / \epsilon_c$, $e_\psi = (e_1 - e_3)s - \epsilon_a c\, e_\rho /4\pi$, $1/\tau = 4\pi \sigma_c/\epsilon_c$, $\sigma_\psi = (\sigma_a - \sigma_c \epsilon_r)c$, $\rho_2 = (e_1 + e_3)s\, c\, q^2$ and $\epsilon_r = \epsilon_a/\epsilon_c$.

Following Smith **et al.[3]** we solve the problem for the case of square wave excitation. The coefficient in **Eqs.(6-8)** now become constants within each half cycle of the applied field and this simplifies the problem considerably. For square wave excitation

$$E_a(t) = \begin{cases} +E & \text{for } 0 < t < 1/2f \\ -E & \text{for } 1/2f < t < 1/f. \end{cases}$$

where **f** is the frequency. The solutions are assumed to be

$$\psi(t) = C_1 \exp(\lambda t/\tau) ,$$
$$\Phi(t) = C_2 \exp(\lambda t/\tau) \quad \text{and}$$
$$Q(t) = C_3 \exp(\lambda t/\tau).$$

Substituting these in Eqs. (6-8) the following characteristic equation of the system is obtained.

$$\lambda^3 (1/\tau^3) + \lambda^2 [\, 1/\tau^3 + 1/(\tau^2 T_\phi) + 1/(\tau^2 T_\psi)]$$
$$+ \lambda [\, 1/(\tau^2 T_\phi) - e_\rho \rho_2 /(\gamma_1 \tau^2) + 1/(\tau^2 T_\psi) + 1/(\tau T_\psi T_\phi)$$
$$- e_\psi \rho_1 E^2/(\eta_2 \gamma_1 \tau) - A \sigma_\psi E^2/(\eta_2 \tau)] + 1/(\tau T_\psi T_\phi)$$
$$- e_\rho \rho_2 /(\gamma_1 \tau T_\psi) - \rho_1 e_\psi E^2/(\eta_2 \gamma_1 \tau) + \rho_1 \sigma_\psi e_\rho E^2/(\eta_2 \gamma_1)$$
$$- A \sigma_\psi E^2/(\eta_2 T_\phi) + A e_\psi \rho_2 E^2/(\eta_2 \gamma_1 \tau) = 0 \qquad (9)$$

The general solutions are:

$$\psi(t) = \sum_{j=1}^{3} a_j \exp(\lambda_j t/\tau) ,$$

$$\Phi(t) = \sum_{j=1}^{3} b_j \exp(\lambda_j t/\tau) , \qquad (10)$$

$$Q(t) = \sum_{j=1}^{3} c_j \exp(\lambda_j t/\tau).$$

where λ_1, λ_2 and λ_3 are the roots of Eq.(9),

$b_j = (T_\phi / d_j T_\psi)[\tau T_\psi A e\psi E^2 - \eta_2 e_\rho (\lambda_j T_\psi + \tau)] a_j$

$c_j = [\{\eta_2 \gamma_1 (\lambda_j T_\phi + \tau)(\lambda_j T_\psi + \tau) - \tau^2 T_\psi T_\phi \rho_1 e_\psi E^2\}/(d_j \tau T_\psi)] a_j$

$d_j = [\tau T_\phi e_\rho \rho_1 E - \gamma_1 A E (\lambda_j T_\phi + \tau)]$

It is clear from Eqs.(6-8) that when E_a changes sign after every half cycle, either Φ and Q should reverse their signs with ψ retaining its sign or ψ should reverse

its sign with Φ and Q retaining their signs. Thus there are two sets of solutions possible corresponding to two regimes of instability, as in the Orsay model [2,3]. In the conduction regime Φ and Q oscillate with the field and ψ does not., ie,

$$\begin{aligned} \psi(t + 1/2f) &= \psi(t) \\ \Phi(t + 1/2f) &= -\Phi(t) \\ Q(t + 1/2f) &= -Q(t). \end{aligned} \tag{11}$$

In the dielectric regime, on the other hand, ψ oscillates with the field and Φ and Q do not.,ie,

$$\begin{aligned} \psi(t + 1/2f) &= -\psi(t) \\ \Phi(t + 1/2f) &= \Phi(t) \\ Q(t + 1/2f) &= Q(t) \end{aligned} \tag{12}$$

In order to obtain the threshold of the instability we have to find a set of eigenvalues λ_1, λ_2 and λ_3 of Eq.(9) that satisfy one of the two conditions corresponding to the two regimes of instability. As it is difficult to get analytical solutions of a cubic equation, we solve the problem numerically. For a given set of values of the material parameters and for a given frequency, we choose some values of a and the applied voltage V_a and find the

eigenvalues of Eq.(9). The voltage V_a is then varied till the λ's satisfy either Eq.(11) or Eq.(12). This value of V_a is the threshold voltage V_{th} for the particular value of a chosen. The calculaions are repeated for different, values of a and V_{th} is obtained as a function of a. The minimum value of V_{th} gives the critical voltage V_c at which the instability sets in and the corresponding value of a gives the tilt of the rolls at the threshold, for the particular value of the frequency chosen. The above process is repeated for different values of the frequency of the applied field.

5.3 RESULTS AND DISCUSSION

The variations of the critical voltage V_c and the corresponding value of a with frequency, calculated for the standard values of the MBBA parameters (see table 1, chapter 3)are shown in Fig. 2. The curves labled (a), (b) and (c) correspond to the onset of the conduction regime, the restabilization branch and the dielectric regime, respectively (see chapter 2, section 4). The dashed lines in the upper section of the figure denote regions in the stability diagram characterized by non-zero values of a. The conduction regime sets in at a critical voltage, which in the one-dimensional model is minimized for $q = 0$. However, using the Helfrich criterion [1] we can take

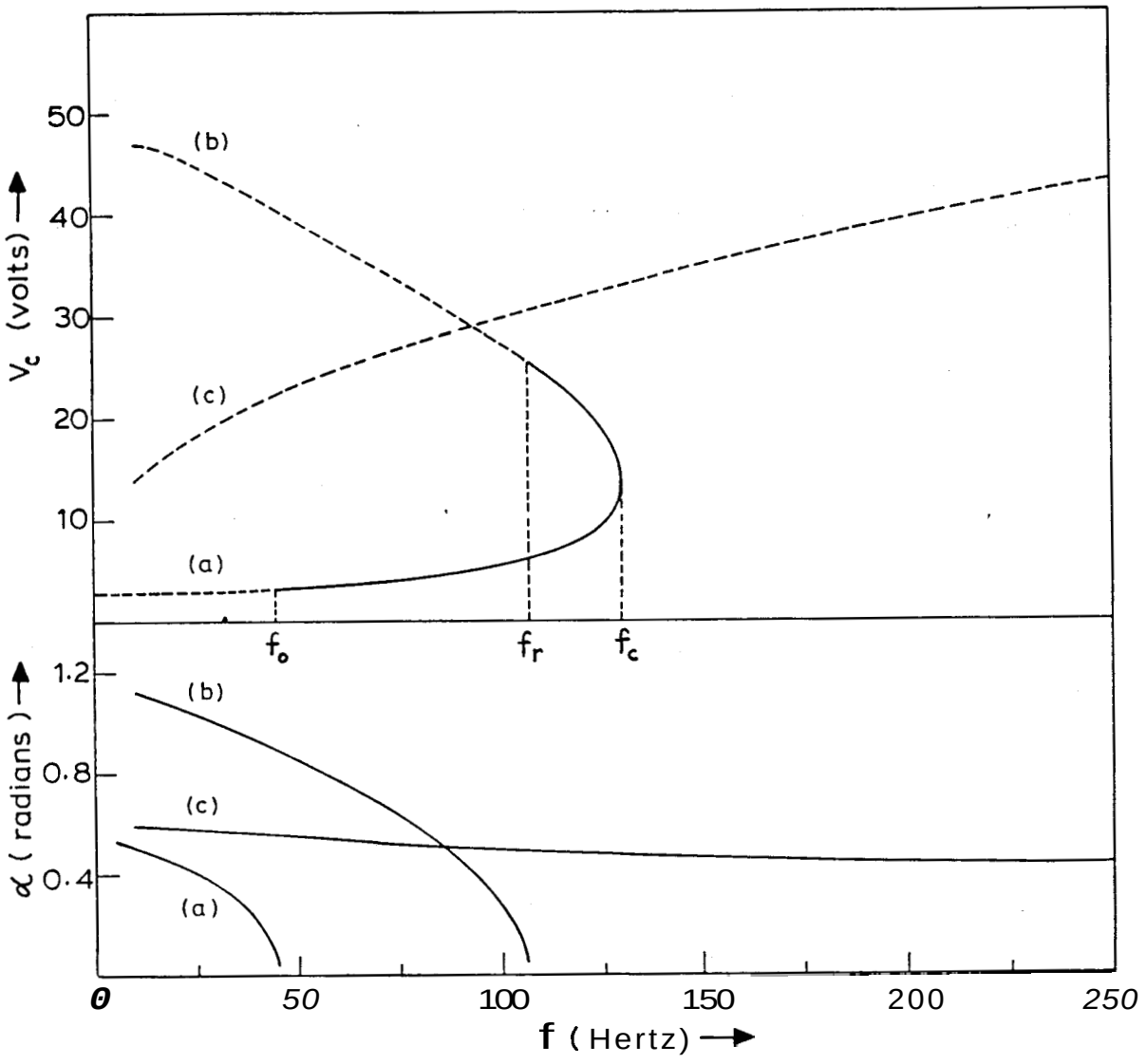

Fig.2. Upper section: Threshold voltage (curve a) and the restabilization voltage (curve b) as a function of the frequency in the conduction regime for MBBA with $\sigma_{\perp} = 3 \times 10^{-10}$ ohm^{-1} cm^{-1}. The low frequency portions indicated by dashed lines are characterized by nonzero values of a. The frequency dependence of the voltage at the threshold for a 20 μm thick sample in the dielectric regime is shown in curve c. Lower section: variation of the tilt angle a of the oblique rolls with frequency. a, b and c correspond to the same branches as in the upper section.

$q = \pi/d$ at the threshold. In the conduction regime oblique rolls are obtained at the threshold upto a critical frequency f_o . Beyond f_o normal rolls occur at the threshold. The conduction regime is obtained only upto a cut-off frequecy $f_c \approx 1/\tau = 4\pi\sigma_{11}/\epsilon_{11}$. The restabi1ization branch is characterized by a field threshold and as at the onset of the conduction regime, q is taken to be equal to π/d. Along this branch oblique rolls occur upto a requency $f_r > f_o$. Therefore in the frequency range $f_o < f < f_r$, though normal rolls occur at the threshold of the conduction regime, oblique rolls can be expected to occur at higher fields.

The dielectric regime is also characterized by a field threshold with $q >> \pi/d$. For the standard values of the material parameters of MBBA, used in the calcalations, oblique rolls are found at all frequencies. However, if the flexoelectric coefficients are decreased by a factor S, keeping the ratio $(e_1 - e_3) / (e_1 + e_3)$ constant at the MBBA value, oblique rolls are obtained only if $S > 0.74$ (Fig.3).

Fig.4a shows the evolution of ψ, Φ and Q for one cycle of the applied field just above the threshold of the conduction regime. Let the three variables be positive and

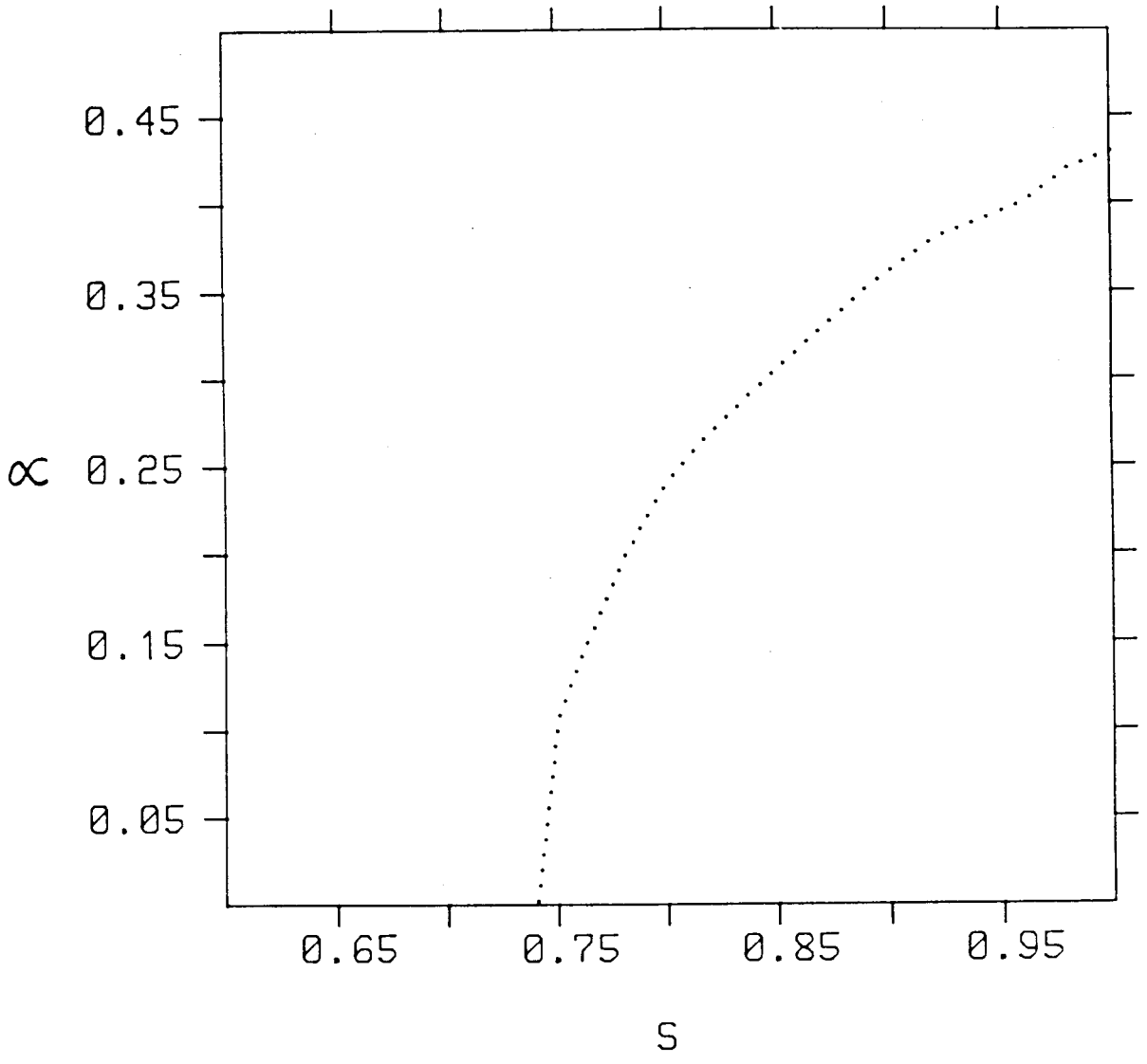

Fig.3. Variation of a (in radians) with the factor S by which the flexoelectric coefficients are decreased, keeping the ratio $(e_1 - e_3)/(e_1 + e_3)$ fixed at the standard MBBA value.

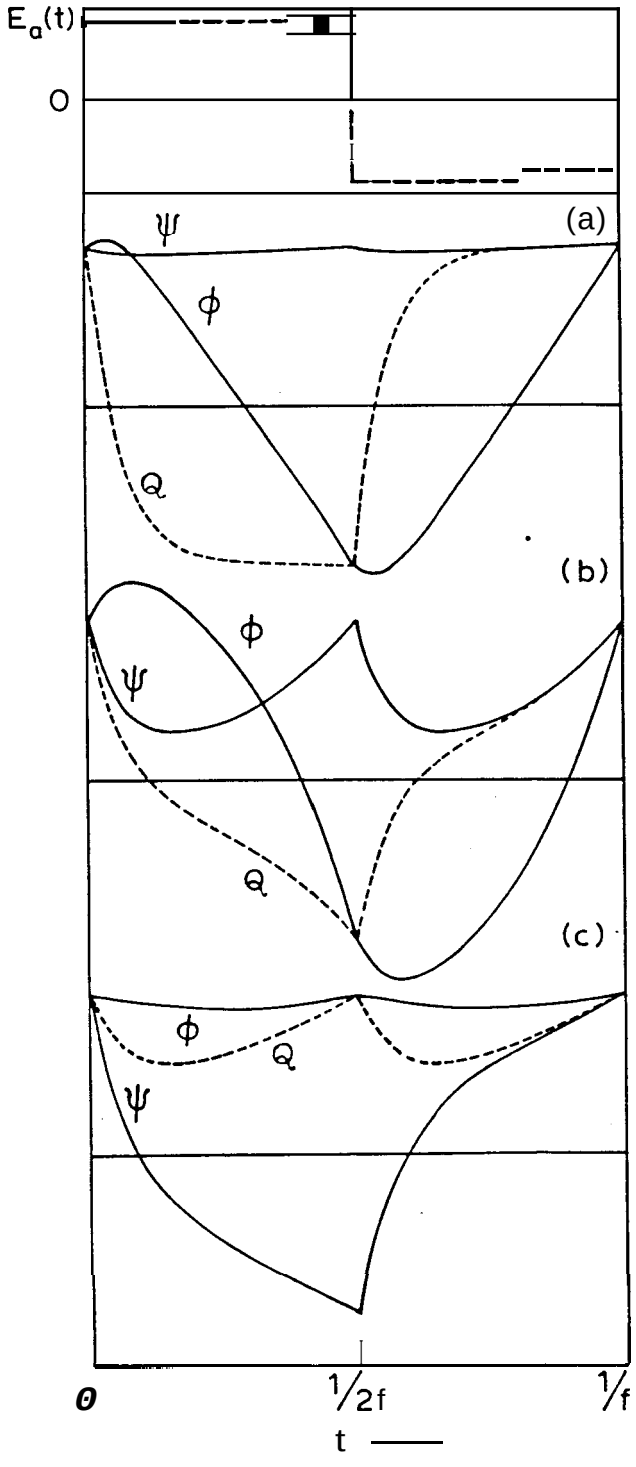

Fig.4. Variation of ψ, Φ and Q with time for one period of the applied square wave field: (a) just above the threshold in the conduction regime at 40 Hz, (b) slightly below the restabilization curve at 100 Hz and (c) in the dielectric regime at 170 Hz. The values of the material parameters used in these calculations are the same as in Fig.2.

increasing at t=0, when the field is reversed. Both source terms in Eq.(6) now change sign and ψ starts to decrease. In Eq.(7) only the ψ term changes sign immediately and since the Q term is stonger than the ψ term, 4 continues to increase. In Eq.(8) the Φ term is negligible and Q also starts to decrease as the ψ term has changed sign. In the conduction regime Q has the shortest relaxation time and hence Q crosses zero before ψ. Once Q is negative the source term containing Q in Eq.(6) regains its initial sign and ψ starts to increase. The influence of the 4 term on the evolution of ψ is found to be negligible. When Q becomes negative the second source term in Eq.(7) also changes sign and Φ decreases and changes sign. Thus Q and Φ oscillate with the applied field. The evolution of these variables near the restabilization branch (Fig.4b) is similar to that at the threshold of the conduction regime. However, since the ψ relaxation time T_ψ is now not very much greater than the charge relaxation time τ, the initial decrease in ψ is much sharper. Along the dielectric regime (Fig.4c), $T < \tau$ and ψ oscillates with the applied field. Since Φ does not oscillate in the dielectric regime, the value of a at the threshold is not very sensitive to the frequency.

It should be noted that the relaxation frequency of

the Φ distortion, $1/T_\phi$, is independent of the applied electric field and typically of the order of a few Hz (see Eq.(7)). Therefore it is clear from the above discussion that Φ is driven and made to oscillate in the conduction regime mainly by the Q term in Eq. (7). Hence if the conductivity of the sample is increased the charge relaxation time would decrease and Φ will be forced to oscillate at higher frequencies. Fig.5 shows the variation of f_o/f_c (curve a) and f_r/f_c (curve b) with $a_{,,}$ for fixed $a_{,}/\sigma_\perp$. For small values of $a_{,,}$, f_r/f_c decreases much more stongly than f_o/f_c, whereas at higher values of σ_{11} their rates of decrease are comparable.

This model also offers a possible explanation of the low frequency EHD instability observed in nematics close to the nematic - smectic (A or C) transition point, having negative conductivity anisotropy (see chapter 2). We have taken a positive value of α_3 since, it is known to be positive in such materials [4]. Taking $a_{,} = 0.5$ poise, $\sigma_a = -0.3\times10^{-10}$ ohm^{-1} cm^{-1} and $\epsilon_a = -0.2$, we find solutions corresponding to the dielectric regime, but not those corresponding to the conduction regime. The instability is found to be characterized by a threshold field, which is minimized for $q = 0$. Therefore using the Helfrich criterion $q = \pi/d$, we get the width of the rolls at threshold to be

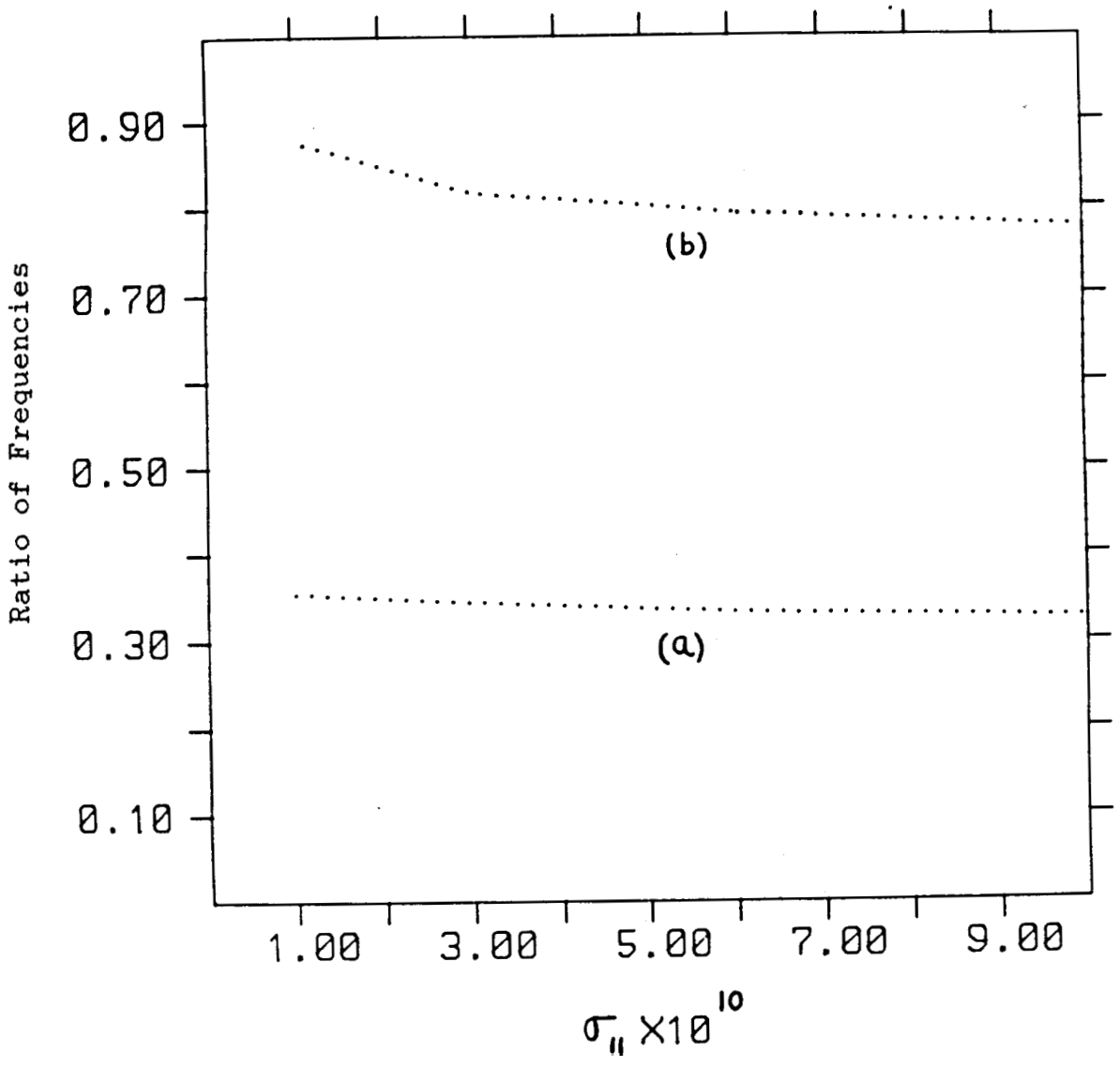

Fig.5. Variation of the ratios of frequencies f_o/f_c (curve a) and f_r/f_c (curve b) with $a_{,,}$ (in $ohm^{-1}cm^{-1}$).

equal to the sample thickness. The value of **a** at the threshold **is** found to be $\approx$ 90' and does not vary much with the frequency of the applied field. The dependence of the threshold field on the frequency is similar to that in the dielectric regime of nematics with $\sigma_a > 0$ (see Fig.2). **It** is clear that in this case the space charge formation is entirely due to the flexoelectric effect, which also accounts for the large value of **a.**

We do not find solutions corresponding to the high frequency regime where $q >> \pi/d$. Here **it** should **be** noted that at high frequencies the experimental value of a_2 will have a positive contribution from the dielectric losses associated with the relaxation of $\varepsilon_{\perp}$. As shown by Goossens [7], this contribution can cause EHD instabilities at relatively high frequencies. The EHD instabilities found in nematics where ϵ_a changes sign at some value of the frequency of the applied field due to the relaxation of $\varepsilon_{\perp}$ [8,9], are understood in terms of the model of Goossens. **It** is possible that in materials with negative conductivity anisotropy at low frequencies, the effective σ_a is actally positive at high frequencies due to the contribution from the dielectric loss of $\varepsilon_{\perp}$. Then these materials can be expected to show an instability similar to the dielectric regime of nematics with positive a_2. The

experimental observation (see chapter 2) that the high frequency regime smoothly goes over to the dielectric regime as the temperature is increased, supports this view.

5.4 COMPARISON WITH EXPERIMENTAL RESULTS

Though oblique rolls at the threshold in the conduction regime have been reported by some authors [10], the only detailed experimental study on these is that of Ribotta et al.[11] (see chapter 2). The stability diagram found experimentally by them is reproduced in Fig.6 . The material used by them is a commercially available nematic mixture (Merck phase V). A detailed comparison of the experimental results with the theory is not possible as many of the material parameters of this mixture are not known. From the figure we see that oblique rolls are found upto a critical frequency f_o with $f_o/f_c \approx 0.3$. Beyond f_o though normal rolls are obtained at the threshold, oblique rolls are found at higher fields. All these features are in agreement with the theoretical results discussed above. However, a non-linear analysis is needed to predict the transition of normal rolls to oblique ones at frequencies beyond f_o . Ribotta et al. [11] also find f_o to increase with the conductivity of the sample, as found from our calculations.

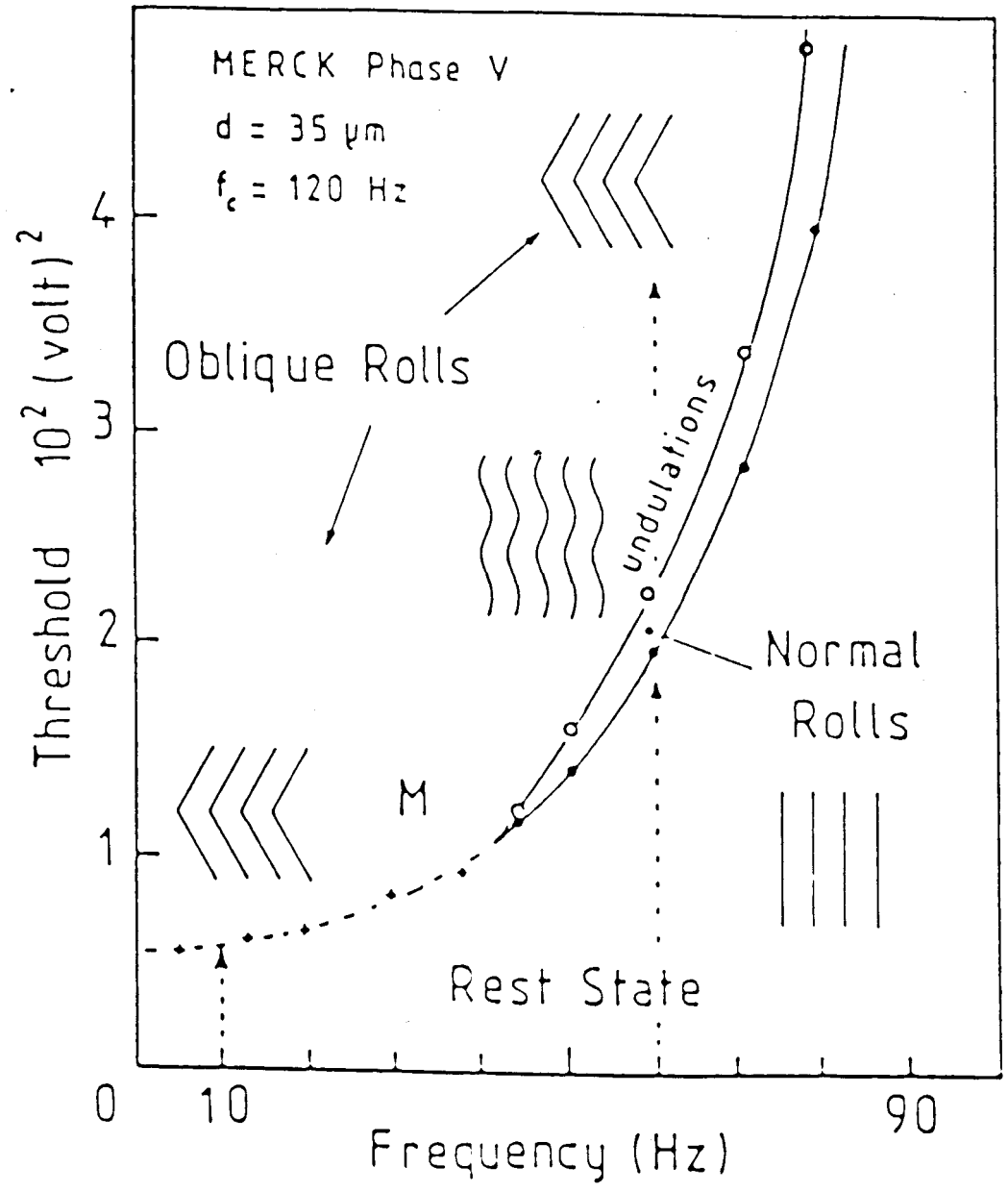

Fig.6. The stability diagram obtained from the experiments of Ribotta et al. [12]. Below the triple point M oblique rolls are obtained at the threshold. Beyond M, normal rolls are obtained at the threshold and as the field strength is further increased, they first become undulatory and then change continuosly into oblique rolls.

Studies on EHD instabilities in MBBA [12] show that in the dielectric regime normal rolls occur at the threshold. If the field is slightly increased the chevron pattern consisting of oblique rolls is obtained. As mentioned in the previous section if the flexoelectric coefficients are decreased slightly our calculations give normal rolls at the threshold of the dielectric regime (Fig.3). Therefore it is likely that the values of the flexoelectric coefficients that we have used are slightly overestimated.

In the experimental studies on EHD instabilities in nematics with $\sigma_a < 0$, discussed in chapter 2 [4,5,6], almost longitudinal domains are found with $q \approx \pi/d$ at the threshold of the low frequency regime. Further, the light scattering experiments of Goscianski [4] show that the curvature of the director oscillates with the applied field in these rolls. These features are in agreement with the results of the calculations, presented in the previous section. Blinov et al. [6] find that at very low frequencies (<20 Hz) The threshold field varies as $\sigma^{1/2}$, σ being the average conductivity of the sample. This feature is not predicted by our model. The isotropic mechanism [6], which gives such a dependence may, therefore, make an important contribution at these low frequencies.

Thus the inclusion of the flexoelectric terms in the EHD equations describing the response of a homogeneously aligned nematic to an external electric field offers a satisfactory explanation of many experimental observations which cannot be accounted for by the earlier models.

REFERENCES

1. W. Helfrich, J. Chem. Phys., 51, 4092 (1969).
2. E. Dubois-Violette, P.G. de Gennes and O. Parodi, J. de Phys., 32, 305 (1971).
3. I.W. Smith, Y. Galerne, S.T. Lagerwall, E. Dubois-Violette and G. Durand, J. de Phys., 36, C1-237 (1975).
4. M. Goscianski, Philips Res. Reports, 30, 37 (1975).
5. M. Goscianski and L. Leger, J. de Phys., 36, C1-231 (1975).
6. L.M. Blinov, M.I. Barnik, V.T. Lazareva and A.N. Trufanov, J. de Phys., 40, C3-263 (1979).
7. W.J.A. Goossens, Phys. Lett., A40, 95 (1972).
8. W.H. de Jeu, C.J. Gerritsma, P. van Zanten and W.J.A. Goossens, Phys. Lett., A39, 355 (1972).
9. W.H. de Jeu and Th.W. Lathouwers, Mol. Cryst. Liq. Cryst., 26, 235 (1974).
10. C. Hilsum and F.C. Saunders, Mol. Cryst. Liq. Cryst., 64, 25 (1980).
11. R. Ribotta, A. Joets and L. Lei, Phys. Rev. Lett., 56, 1595 (1986).
12. Orsay liquid crystals group, Mol. Cryst. Liq. Cryst., 12, 251 (1971).